 CMES, vol.87, no.5, pp.461-481, 2012

Elasto-Damage Modeling of Biopolymer Molecules Response

F. Maceri[1], **M. Marino**[1] **and G. Vairo**[1]

Abstract: The mechanical behavior of biopolymer molecules is herein addressed and a novel predictive model for their elasto-damage response is proposed. Both entropic and energetic elastic mechanisms are accounted for, and coupled by consistent equilibrium conditions. Moreover, through non-smooth mechanics arguments, molecular damage is modeled accounting for failure due to both mechanical and non-mechanical damage sources. The model is applied to collagen molecules and an excellent agreement with available experimental tests and atomistic computations is shown. The proposed predictive theory can be usefully integrated in hierarchical models of biological structures towards a multiscale continuum approach.

Keywords: Elasto-damage models; Biopolymer molecules; Entropic and energetic elasticity; Non-smooth mechanics; Hierarchical multiscale modeling; Tropocollagen molecules

1 Introduction

Biopolymer molecules (that is polynucleotides, polysaccharides, and polypeptides) have a complex non-linear mechanical response due to the interaction between entropic and energetic mechanisms (MacKintosh, Käs, and Jamney, 1995; Wang, Yin, Landick, Gelles, and Block, 1997; Buehler and Wong, 2007; Holzapfel, and Ogden, 2010). Establishing a sound mechanical model of single biopolymer molecules is a milestone in the understanding of fundamental processes in molecular biology and biomechanics. For instance, mechanics of DNA or lipid membranes highly affect cellular physiological functions (Wang, Yin, Landick, Gelles, and Block, 1997; Rawicz, Olbrich, McIntosh, Needham, and Evans, 2000) as well as pathological mechanisms in cells are often strictly related with damage of these biopolymer

[1] Department of Civil Engineering, University of Rome "Tor Vergata", Via del Politecnico 1, 00133 Rome Italy, E-mail: franco.maceri@lagrange.it, m.marino@ing.uniroma2.it, vairo@ing.uniroma2.it

molecules (Pagán and Mackey, 2000; Jackson and Bartek, 2009).

Moreover, mechanics of biological cells, tissues, and organs mainly depends on structural proteins (mostly fibrous proteins) such as actin in cells (Unnikrishnan, Unnikrishnan, and Reddy, 2007), collagen in connective tissues (Fratzl, 2008), and titin in muscles (Linke, Iveyemer, Mundel, Stockmeier, and Kolmerer, 1998). Constitutive hyperelastic, visco-elastic or visco-elasto-damage models of biological structures can be developed within a phenomenological (Fung, 1981), structural (Holzapfel, and Gasser, 2007), or structural multiscale (Maceri, Marino, and Vairo, 2010a) framework. Within the structural approach, micromechanical effects are usually treated through micro-macro approaches, allowing to derive constitutive response and damage evolution at the macroscale starting from the behavior of microscale structures. At the microscale, material is usually described by the phenomenological choice of a suitable hyperelastic law (Holzapfel, Gasser, and Stadler, 2002; Humphrey, 2002). On the other hand, in a structural multiscale framework, microscale material non-linearities are included by upscaling the mechanical behavior of the nanoscale constituents, that is biopolymer molecules for biological structures, leading to a nano-micro-macro approach. Such a multiscale modeling technique has been successfully applied to describe the elastic response of soft collagenous tissues (Maceri, Marino, and Vairo, 2010a; Marino and Vairo, 2012), as well as for predicting damage effects in different structural contexts (Pichler and Hellmich, 2011). Thereby, the starting point for nano-micro-macro approaches is the modeling accuracy of the mechanical behavior of biopolymer molecules.

Evidences at the nanoscale are of major importance in order to assess the best modeling choices for both elastic and damage behavior of macromolecules. Several experimental techniques, such as atomic force microscopy and optical tweezers, are available and have been used (Wang, Yin, Landick, Gelles, and Block, 1997; Sun, Luo, Fertala, and An, 2002; Bozec and Horton, 2005). Moreover, atomistic theoretical formulation and numerical techniques (e.g., molecular dynamics simulation, MDS) have been recently employed in order to account for atomistic mechanisms affecting molecular deformation and rupture (de Leeuw, 2004; Buehler, 2008; Pradhan, Katti D., and Katti K., 2011).

There is a great need for analytical approaches able to describe mechanics of biopolymer molecules allowing to develop continuum-based models of biological structures. In fact, the simulation of DNA or biological membranes over length and time scales relevant to cellular biology is not currently feasible using conventional simulation strategies at the atomistic scale. This is due to the very high computational cost of such simulations which can be in some cases lowered employing molecular coarse grain representations (Ayton and Voth, 2010). Moreover, address-

ing structural proteins aiming to develop nano-micro-macro models of tissues, the challenge is to upscale molecular properties allowing to account for the interactions of materials across scales and multiscale damage effects.

In this paper, a predictive theory for the elasto-damage behavior of biopolymer molecules is developed, accounting for both entropic and energetic elastic regimes. Molecular damage is modeled by means of non-smooth mechanics arguments in the framework of an internal-constrained approach (Frémond, 2002; Moreau, 2003), and thereby damage evolution due to loads or external sources is described by a non-classical but simple law, depending on few parameters with a clear physical meaning.

Addressing collagen (i.e., the most abundant protein in the human body) and in order to assess the soundness and the accuracy of the proposed predictive theory, several parametric analyses are carried out. The model is validated by comparing obtained results with experimental tests and atomistic computations. Moreover, through an inverse-like scheme and in the case of collagen, the range of values for model parameters is provided.

2 Experimental and numerical evidences

The mechanical behavior of macromolecules is a consequence of a complex interaction between thermal fluctuations (addressed as a source of entropic elasticity) and stretching of covalent bonds (energetic or enthalpic elasticity). Both theoretical (MacKintosh, Käs, and Jamney, 1995) and computational (Buehler, 2006) results indicate that thermal fluctuations dominate molecular mechanical response when the end-to-end molecular length ℓ_m is very small in comparison with the molecular contour length ℓ_c. Dealing only with entropic mechanisms, a well-established approach is represented by the Worm-Like Chain (WLC) model which regards molecules as isotropic continuously flexible rods (Marko and Siggia, 1995; MacKintosh, Käs, and Jamney, 1995). In agreement with the WLC model, an interpolation formula that describes the relationship between ℓ_m and the along-the-chord force F^s applied at molecular ends is

$$F^s(\ell_m) = \rho \left[\frac{1}{4\,(1-\ell_m/\ell_c)^2} - \frac{1}{4} + \frac{\ell_m}{\ell_c} \right] \tag{1}$$

where $\rho = k_B T/\ell_p$, T being the absolute temperature, k_B the Boltzmann constant, and ℓ_p the molecular persistence length (that is, the maximum contour length over which the molecule will appear straight in the presence of thermal undulations). Eq. 1 exhibits a pole for $\ell_m = \ell_c$, describing the inability of extending the end-to-end molecular length over ℓ_c only by involving entropic mechanisms. Nevertheless,

when ℓ_m approaches ℓ_c, the applied force contributes to activate the stretching of covalent bonds, indicating the onset of energetic mechanisms (MacKintosh, Käs, and Jamney, 1995; Buehler, 2006). This is the case of DNA and collagen molecules, for which experiments show a significant degree of molecular extensibility behind ℓ_c (Wang, Yin, Landick, Gelles, and Block, 1997; Sun, Luo, Fertala, and An, 2002). Theoretical models accounting for molecular compliance have been recently proposed (Wang, Yin, Landick, Gelles, and Block, 1997; Holzapfel, and Ogden, 2010). In these approaches, the transition from entropic to energetic mechanisms is not explicitly modelled and, thereby, it is regulated in a phenomenological way.

Collagen molecules in biological tissues are characterized by hydroxyproline-deficient sequences, referred to as labile domains and indicated as molecular kinks, whose length ℓ_{kinks} is about 20 nm. Since ℓ_{kinks} is comparable with the value of the persistence length ℓ_p for collagen (about 14 nm), molecular kinks are activated by thermal fluctuations (Buehler and Wong, 2007; Fratzl, 2008) and represent a source of entropic elasticity for collagen molecules within fibrils in biological tissues. The transition from entropic towards energetic elasticity for collagen has been recently investigated by Buehler and Wong (2007) using MDS approaches. They numerically predicted, for a molecule with $\ell_c = 301.7$ nm, the transition onset at $\ell_m = 280$ nm and its completion at $\ell_m = 317$ nm. Moreover, collagen energetic elasticity is usually modelled by assuming a linearly elastic response (Buehler and Wong, 2007; Maceri, Marino, and Vairo, 2010a). Nevertheless, as experimental (Sun, Luo, Fertala, and An, 2002) and MDS-based (Buehler, 2006; Gautieri, Buehler, and Redaelli, 2009) results suggest, the mechanical response of collagen molecules due to energetic effects is highly non-linear and tends asymptotically towards a linearly elastic behavior for $\ell_m >> \ell_c$. This is essentially due to the unrolling mechanisms of the triple helical structure, characterizing a collagen molecule and tending to disappear when $\ell_m >> \ell_c$. Moreover, for high values of ℓ_m molecular damage is experienced. In this context, Buehler (2006) numerically obtained the ultimate response of isolated tropocollagen segments indicating the damage onset for ℓ_m in the range $1.37\,\ell_c - 1.50\,\ell_c$.

3 Elasto-damage nanomechanical model

The elasto-damage behavior of a biopolymer molecule is herein described by involving arguments of convex analysis (Moreau, 2003), and defining suitable expressions for the free-energy and the pseudo-potential of dissipation. In this formulation, any inertial and viscous effect is disregarded.

The internal-constrained approach introduced by Frémond (2002) and Moreau (2003), is employed to enforce some physical restrictions on the values of the molecular state quantities, by using indicator functions and subdifferential sets. In the fol-

lowing, denoting with K a convex set in $\mathbb{R}$, the indicator function of K is defined as

$$\mathrm{I}_K(x) = \begin{cases} 0 & \text{if } x \in K \\ +\infty & \text{else} \end{cases}, \tag{2}$$

and its subdifferential set results in

$$\partial \mathrm{I}_K(x) = \begin{cases} \{-\alpha^2 \,|\, \alpha \in \mathbb{R}\} & \text{if } x = \inf(K) \\ 0 & \text{if } x \in \mathring{K} \\ \{\alpha^2 \,|\, \alpha \in \mathbb{R}\} & \text{if } x = \sup(K) \\ \nexists & \text{else} \end{cases}. \tag{3}$$

being $\mathring{K}$ the interior of K.

Furthermore, as a notation rule, t denotes the time-variable and $\dot{x}$ the time derivative of x.

A molecule is modeled as an equivalent zero-dimensional nano-structure whose reference end-to-end length is $\ell_{m,o} < \ell_c$ and with A_m as cross-sectional area measure. Let $\varepsilon_m = (\ell_m/\ell_{m,o} - 1)$ be the molecular nominal strain measure and β_m the dimensionless time-dependent function, valued in $[0,1]$, that measures molecular damage due to rupture of covalent bonds. Accordingly, $\beta_m = 1$ indicates a sound molecule, $\beta_m \in (0,1)$ refers to a partially-damaged molecule, and $\beta_m = 0$ means that the molecule is fully cracked. It is worth pointing out that ε_m gives a measure of variations in nanoscale configuration, and β_m is associated with sub-nanoscale motions, not directly affecting nanoscale molecular kinematics.

Entropic and energetic mechanisms are assumed to act as in series and they contribute to the overall molecular stretch measure ε_m by ε_m^s and ε_m^h, respectively, such that by compatibility

$$\varepsilon_m = \varepsilon_m^s + \varepsilon_m^h. \tag{4}$$

Accordingly, both mechanisms induce variations in molecule configuration, but only the energetic one (related to ε_m^h) produces the extension of its covalent bonds. Therefore, damage occurrence is assumed to be controlled only by ε_m^h.

3.1 Free-energy and pseudo-potential of dissipation

Assuming quantities $(\varepsilon_m^s, \varepsilon_m^h, \beta_m)$ as state variables, the molecular free-energy density is herein defined as:

$$\Psi_m(\varepsilon_m^s, \varepsilon_m^h, \beta_m) = \Psi_m^s(\varepsilon_m^s) + \beta_m \Psi_m^h(\varepsilon_m^h) + (1-\beta_m) w_m + \mathrm{I}_{[0,1]}(\beta_m), \tag{5}$$

where w_m indicates a threshold level for damage activation. Moreover, by letting $r_\ell = \ell_{m,o}/\ell_c$, we assume that the entropic contribution Ψ^s_m is

$$\Psi^s_m(\varepsilon^s_m) = \frac{\rho}{A_m}\left\{\frac{1}{4[1-r_\ell(1+\varepsilon^s_m)]r_\ell} - \frac{\varepsilon^s_m}{4} + r_\ell\varepsilon^s_m\left(\frac{\varepsilon^s_m}{2}+1\right)\right\} - \sigma^s_o\varepsilon^s_m - \Psi^s_o\,, \tag{6}$$

and the energetic one Ψ^h_m is

$$\Psi^h_m(\varepsilon^h_m) = \frac{\hat{E}}{r_\ell}\left[\frac{g(1+e^{k(\varepsilon^h_o - r_\ell\varepsilon^h_m)})}{k^2} + \frac{(r_\ell\varepsilon^h_m - \varepsilon^h_o)^2}{2}\right] + \frac{\hat{E}_o r_\ell(\varepsilon^h_m)^2}{2} - \sigma^h_o\varepsilon^h_m - \Psi^h_o\,, \tag{7}$$

where $\hat{E}$, $\hat{E}_o$, ε^h_o and k indicate material parameters of the model and the following positions are made

$$\sigma^s_o = \frac{\rho}{A_m}\left[\frac{1}{4(1-r_\ell)^2} - \frac{1}{4} + r_\ell\right], \qquad \Psi^s_o = \frac{\rho}{4A_m r_\ell(1-r_\ell)}\,, \tag{8}$$

$$\sigma^h_o = \frac{\hat{E}\log(1+e^{-k\varepsilon^h_o})}{k}\,, \qquad \Psi^h_o = \frac{\hat{E}}{r_\ell}\left[\frac{g(1+e^{k\varepsilon^h_o})}{k^2} + \frac{(\varepsilon^h_o)^2}{2}\right], \tag{9}$$

$g(x)$ being the dilog function:

$$g(x) = \mathrm{dilog}(x) = \int_1^x \frac{\log t}{1-t}\mathrm{d}t\,. \tag{10}$$

Eq. 6 allows to recover the WLC model (see Eq. 1) by considering, in agreement with standard arguments of an hyperelastic framework, the first derivative of the entropic free-energy contribution with respect to ε^s_m

$$F^s(\ell_{m,o} + \bar{\varepsilon}^s_m\ell_{m,o}) - F^s(\ell_{m,o}) = A_m\left.\frac{\partial\Psi^s_m}{\partial\varepsilon^s_m}\right|_{\bar{\varepsilon}^s_m}\,, \tag{11}$$

whereas, as a result of the position in Eq. 7, a molecular tangent elastic response in the energetic regime, characterized by an asymptotic linearly elastic behavior and consistent with both experimental and numerical evidences (see Section 2), is obtained by

$$\frac{\partial^2\Psi^h_m}{\partial{\varepsilon^h_m}^2} = \frac{\hat{E}r_\ell}{1+e^{-k(r_\ell\varepsilon^h_m - \varepsilon^h_o)}} + \hat{E}_o r_\ell = E^h_m(\varepsilon^h_m)\,. \tag{12}$$

Since the possible damage occurrence, the evolution of the molecular response -described by $(\dot{\varepsilon}^s_m, \dot{\varepsilon}^h_m, \dot{\beta}_m)$- is affected by the choice of the pseudo-potential of dissipation Φ_m. In order to model different damage rules (DR 1 and DR 2), two

descriptions are employed:

$$\Phi_m(\dot{\varepsilon}^s_m, \dot{\varepsilon}^h_m, \dot{\beta}_m) = \Phi_m(\dot{\beta}_m) = \begin{cases} c_m \dot{\beta}^2_m/2 + \mathrm{I}_{(-\infty,0]}(\dot{\beta}_m) & \text{for DR 1} \\ c_m \dot{\beta}^2_m/2 + \mathrm{I}_{[-v_o,0]}(\dot{\beta}_m) & \text{for DR 2} \end{cases}, \tag{13}$$

where $c_m \in \mathbb{R}^+$ and $v_o \in \mathbb{R}^+$ are model parameters, whose (clear) physical meaning will be shown in the following. It should be remarked that Φ_m is herein assumed to be dependent only on the damage rate and not on the strain rate.

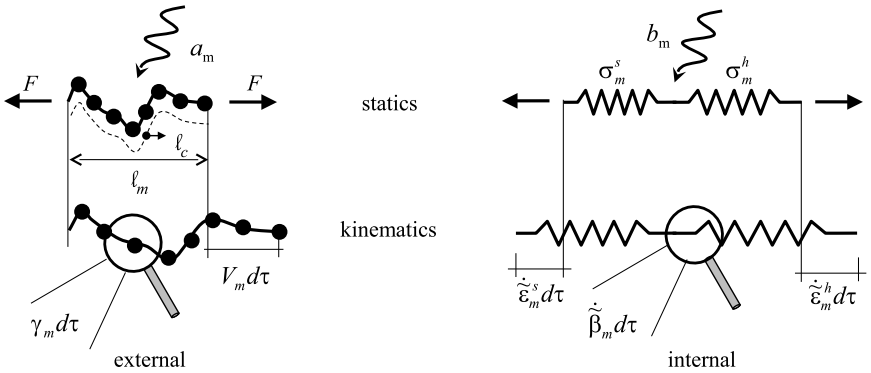

Figure 1: Elasto-damage model: notation.

3.2 Governing equations

The predictive theory of elasto-damage response of biopolymer molecules is derived by applying the Principle of Virtual Powers. To this aim (see Fig. 1), let the internal virtual kinematics be described by $\dot{\tilde{\varepsilon}}^s_m$ and $\dot{\tilde{\varepsilon}}^h_m$ as the entropy- and enthalpy-related virtual strain rates at the nanoscale, respectively, and $\dot{\tilde{\beta}}_m$ as the sub-nanoscale virtual damage rate. Moreover, V_m and γ_m are the virtual velocities relevant to nanoscale and sub-nanoscale configuration changes, respectively, describing the external virtual kinematics. Accordingly, let K_c be the set of kinematically admissible virtual velocities, given by:

$$K_c = \{(V_m, \gamma_m, \dot{\tilde{\varepsilon}}^s_m, \dot{\tilde{\varepsilon}}^h_m, \dot{\tilde{\beta}}_m) \mid V_m = (\dot{\tilde{\varepsilon}}^s_m + \dot{\tilde{\varepsilon}}^h_m)\ell_{m,o}\,, \gamma_m = \dot{\tilde{\beta}}_m\}\,. \tag{14}$$

The internal virtual power for a biopolymer molecule is defined as

$$W^{int}_m = A_m \left(\sigma^s_m \dot{\tilde{\varepsilon}}^s_m + \sigma^h_m \dot{\tilde{\varepsilon}}^h_m\right) \ell_{m,o} + b_m \dot{\tilde{\beta}}_m\,, \tag{15}$$

where σ^s_m and σ^h_m are the molecular stress measures [Nm^{-2}] associated with entropy and enthalpy mechanisms, respectively (i.e., the dual quantities to ε^s_m and ε^h_m), and

b_m [Nm] is the interior sub-nanoscale damage work, representing a non-classical term dual to the damage state quantity β_m (Fig. 1).

The external virtual power is defined as

$$W_m^{ext} = FV_m + a_m\gamma_m\,, \tag{16}$$

where F is the intensity of the self-equilibrated external forces applied at the molecular ends along the molecular end-to-end direction, and a_m is an exterior source of sub-nanoscale work (e.g., due to chemical, electrical, or magnetic sources).

The application of the Principle of Virtual Powers for any set of kinematically admissible virtual velocities, that is

$$W_m^{int} = W_m^{ext} \quad \forall\,(V_m, \gamma_m, \dot{\tilde{\varepsilon}}_m^s, \dot{\tilde{\varepsilon}}_m^h, \dot{\tilde{\beta}}_m) \in K_c\,, \tag{17}$$

gives the equilibrium relationships:

$$\sigma_m^s = \sigma_m^h = \frac{F}{A_m}\,, \tag{18}$$

$$b_m = a_m\,. \tag{19}$$

Static quantities $(\sigma_m^s, \sigma_m^h, b_m)$ and state variables are related through the constitutive laws, defined as

$$\sigma_m^s = \frac{\partial\Psi_m}{\partial\varepsilon_m^s} + \frac{\partial\Phi_m}{\partial\dot{\varepsilon}_m^s}\,, \quad \sigma_m^h = \frac{\partial\Psi_m}{\partial\varepsilon_m^h} + \frac{\partial\Phi_m}{\partial\dot{\varepsilon}_m^h}\,, \quad b_m = \frac{\partial\Psi_m}{\partial\beta_m} + \frac{\partial\Phi_m}{\partial\dot{\beta}_m}\,. \tag{20}$$

Combining Eq. 18, Eq. 19 and Eq. 20, together with Eq. 5 and Eq. 13, the elasto-damage predictive theory results in:

$$\frac{\rho}{A_m}\left\{\frac{1}{4[1-r_\ell(1+\varepsilon_m^s)]^2} - \frac{1}{4} + r_\ell(\varepsilon_m^s+1)\right\} - \sigma_o^s = \\ = \beta_m\left\{\frac{\hat{E}}{k}\left[\log\left(1+e^{k(r_\ell\varepsilon_m^h-\varepsilon_o^h)}\right)\right] + \hat{E}_o r_\ell \varepsilon_m^h - \sigma_o^h\right\} = \frac{F}{A_m} \tag{21}$$

$$c_m\dot{\beta}_m + \Psi_m^h - w_m - a_m + \partial \mathrm{I}_{[0,1]}(\beta_m) + \partial \mathrm{I}_{(-\infty,0]}(\dot{\beta}_m) \ni 0 \qquad \text{for DR 1} \tag{22}$$

$$c_m\dot{\beta}_m + \Psi_m^h - w_m - a_m + \partial \mathrm{I}_{[0,1]}(\beta_m) + \partial \mathrm{I}_{[-v_o,0]}(\dot{\beta}_m) \ni 0 \qquad \text{for DR 2} \tag{23}$$

The analysis of Eq. 22 and Eq. 23 highlights that c_m has the meaning of damage viscosity parameter, and v_o in DR 2 is the upper bound value for the damage rate.

3.3 About well-posedness of damage model

In order to discuss about the well-posedness of the proposed damage model, the damage evolution described by Eq. 22 and Eq. 23 is proved in what follows to be uniquely determined for given values of damage sources.

The definition domains of the subdifferential sets occurring in Eq. 22 and Eq. 23 restrict the range of values for β_m and $\dot{\beta}_m$ to

$$\beta_m \in [0,1]\,, \quad \dot{\beta}_m \in (-\infty, 0] \quad \text{for DR 1}\,, \tag{24}$$

$$\beta_m \in [0,1]\,, \quad \dot{\beta}_m \in [-v_o, 0] \quad \text{for DR 2}\,. \tag{25}$$

Moreover, from Eq. 3, the following explicit rules hold:

$$\partial \mathrm{I}_{[0,1]}(x) = \begin{cases} \{-\alpha^2 \,|\, \alpha \in \mathbb{R}\} & \text{if } x = 0 \\ 0 & \text{if } x \in (0,1) \\ \{\alpha^2 \,|\, \alpha \in \mathbb{R}\} & \text{if } x = 1 \\ \nexists & \text{else} \end{cases}, \tag{26}$$

$$\partial \mathrm{I}_{(-\infty,0]}(x) = \begin{cases} 0 & \text{if } x \in (-\infty, 0) \\ \{\gamma^2 \,|\, \gamma \in \mathbb{R}\} & \text{if } x = 0 \\ \nexists & \text{else} \end{cases}, \tag{27}$$

$$\partial \mathrm{I}_{[-v_o,0]}(x) = \begin{cases} \{-\xi^2 \,|\, \xi \in \mathbb{R}\} & \text{if } x = -v_o \\ 0 & \text{if } x \in (-v_o, 0) \\ \{\xi^2 \,|\, \xi \in \mathbb{R}\} & \text{if } x = 0 \\ \nexists & \text{else} \end{cases}. \tag{28}$$

where the notation employing the square of constants has been introduced to emphasize the intrinsic sign of those constants.

Since $\dot{\beta}_m < 0$ when $\beta_m = 1$ (respectively, $\beta_m = 0$) is not an admissible occurrence because $\dot{\beta}_m < 0$ strictly implies $\beta_m < 1$ (respectively, $\beta_m < 0$), the following cases can be distinguished:

- **Case 1:** $\beta_m \in (0,1]$ and $\Psi_m^h - a_m - w_m = -q^2 \leq 0$. A zero damage rate ($\dot{\beta}_m = 0$) satisfies Eq. 22 for DR 1 (respectively Eq. 23 for DR 2). In fact
  - if $\beta_m \in (0,1]$ and $\dot{\beta}_m = 0$ then there exist $\alpha, \gamma, \xi \in \mathbb{R}$ such that $-q^2 + \alpha^2 + \gamma^2 = 0$ (for DR 1) and $-q^2 + \alpha^2 + \xi^2 = 0$ (for DR 2), that is Eq. 22 and Eq. 23 are satisfied;

– if $\beta_m \in (0,1)$ and $\dot{\beta}_m = \dot{\beta}_m^* \in (-\infty, 0)$ for DR 1 or $\dot{\beta}_m = \dot{\beta}_m^* \in (-v_o, 0)$ for DR 2 then Eq. 22 and Eq. 23 have no solution: $c_m \dot{\beta}_m^* - q^2 \neq 0$.

- **Case 2:** $\beta_m \in (0,1]$ and $\Psi_m^h - a_m - w_m = q^2 > 0$.

  DR 1. In this case the value of the damage rate that satisfies Eq. 22 is $\dot{\beta}_m = -q^2/c_m$. In fact,

  – if $\beta_m \in (0,1]$ and $\dot{\beta}_m = 0$, then Eq. 22 has no solution, that is there does not exist $\alpha, \gamma \in \mathbb{R}$ such that $q^2 + \alpha^2 + \gamma^2 = 0$.

  – if $\beta_m \in (0,1)$ and $\dot{\beta}_m = \dot{\beta}_m^* \in (-\infty, 0) \setminus \{-q^2/c_m\}$, then Eq. 22 has no solution: $c_m \dot{\beta}_m^* + q^2 \neq 0$.

  – if $\beta_m \in (0,1)$ and $\dot{\beta}_m = \dot{\beta}_m^* = -q^2/c_m$, then Eq. 22 is satisfied: $c_m \dot{\beta}_m^* + q^2 = 0$.

  DR 2. In this case, $\dot{\beta}_m = \max\{-q^2/c_m, -v_o\}$ satisfies Eq. 23 for any value $\beta_m \in (0,1]$. In fact,

  – if $\beta_m \in (0,1]$ and $\dot{\beta}_m = 0$, then Eq. 23 has no solution, that is there does not exist $\alpha, \xi \in \mathbb{R}$ such that $q^2 + \alpha^2 + \xi^2 = 0$ for any value of q^2.

  – if $q^2 < c_m v_o$, $\beta_m \in (0,1)$ and $\dot{\beta}_m = \dot{\beta}_m^* \in (-v_o, 0) \setminus \{-q^2/c_m\}$, then Eq. 23 has no solution: $c_m \dot{\beta}_m^* + q^2 \neq 0$.

  – if $q^2 < c_m v_o$, $\beta_m \in (0,1)$ and $\dot{\beta}_m = \dot{\beta}_m^* = -q^2/c_m$, then Eq. 23 is satisfied: $c_m \dot{\beta}_m^* + q^2 = 0$.

  – if $q^2 > c_m v_o$, $\beta_m \in (0,1)$ and $\dot{\beta}_m = \dot{\beta}_m^* = -v_o$, then Eq. 23 is satisfied, that is there exists $\xi \in \mathbb{R}$ such that $-c_m v_o + q^2 - \xi^2 = 0$.

- **Case 3:** $\beta_m = 0$.

  In this case, $\dot{\beta}_m = 0$ satisfies both Eq. 22 and Eq. 23 for $\beta_m = 0$ and for any value of the quantity $\Psi_m^h - a_m - w_m$.

3.4 Purely elastic response

If damage is not activated ($\beta_m = 1$), Eq. 21 represents the equilibrium condition of the series of two nonlinearly elastic springs (associated to entropic and energetic mechanisms, respectively). Therefore, the following molecular tangent modulus can be introduced:

$$E_m(\varepsilon_m) = \frac{E_m^s(\varepsilon_m^s) E_m^h(\varepsilon_m^h)}{E_m^s(\varepsilon_m^s) + E_m^h(\varepsilon_m^h)}, \tag{29}$$

where

$$E_m^s = \frac{\partial^2 \Psi_m^s}{\partial \varepsilon_m^{s\,2}} = \frac{\rho}{A_m} \left\{ \frac{r_\ell}{2[1 - r_\ell(1+\varepsilon_m^s)]^3} + r_\ell \right\}, \tag{30}$$

and E_m^h is expressed by Eq. 12. Strain contributions due to entropic and energetic effects, that is functions $\varepsilon_m^s = \varepsilon_m^s(\varepsilon_m)$ and $\varepsilon_m^h = \varepsilon_m^h(\varepsilon_m)$, are obtained by solving the following differential problem:

$$\dot{\varepsilon}_m^s = \frac{E_m(\varepsilon_m)\dot{\varepsilon}_m}{E_m^s(\varepsilon_m^s)}, \quad \dot{\varepsilon}_m^h = \frac{E_m(\varepsilon_m)\dot{\varepsilon}_m}{E_m^h(\varepsilon_m^h)}. \tag{31}$$

4 Results

The model herein proposed is applied for analysing the elasto-damage response of collagen macromolecules. Referring to tensile tests and considering a displacement-based approach with a constant deformation rate set equal to $\dot{\ell}_m = 1$ mm/min, the model results are compared with experimental (Sun, Luo, Fertala, and An, 2002; Bozec and Horton, 2005) and atomistic computational (Buehler, 2006; Buehler and Wong, 2007; Gautieri, Buehler, and Redaelli, 2009) evidences. It is worth pointing out that the available experimental tests address the purely elastic response of collagen, affected by both entropic and energetic mechanisms, while the numerical results provide also some data on molecular damage. In the following, we consider as constant parameters $A_m = 1.41$ nm^2 and $T = 310$ K.

4.1 Molecular elastic behavior

As regards the molecular elastic response (described by differential problem in Eq. 31 coupled with Eq. 29), only the energetic contribute is firstly addressed. Numerical simulations are performed considering $\ell_{m,o} \to \ell_c$ (i.e., $\ell_{m,o}/\ell_c = 1 - \delta$ with $\delta \in \mathbb{R}^+$ and $\delta << 1$). In this case, thermal fluctuations do not contribute to molecular strain, that is $E_m^s \to +\infty$. In order to justify the modeling choices on Ψ_m^h, both the $F - \varepsilon_m^h$ and $E_m^h - \varepsilon_m^h$ relationships obtained by the present approach are compared with MDS results by Gautieri, Buehler, and Redaelli (2009) performed on short length and straight tropocollagen segments ($\ell_c = 8.4$ nm, see Fig. 2), showing an excellent agreement. As shown in Fig. 2b, values of model parameters, since their physical meaning, can be directly kept from MDS established results.

Addressing both entropic and energetic contributes, in Fig. 3 the computed $F - \ell_m$ curve is compared with the experimental one by Bozec and Horton (2005). The WLC model fits well the low force experimental data but looses validity for high forces. On the contrary, the proposed model takes into account molecular compliance and exhibits an excellent agreement in the overall force range herein ad-

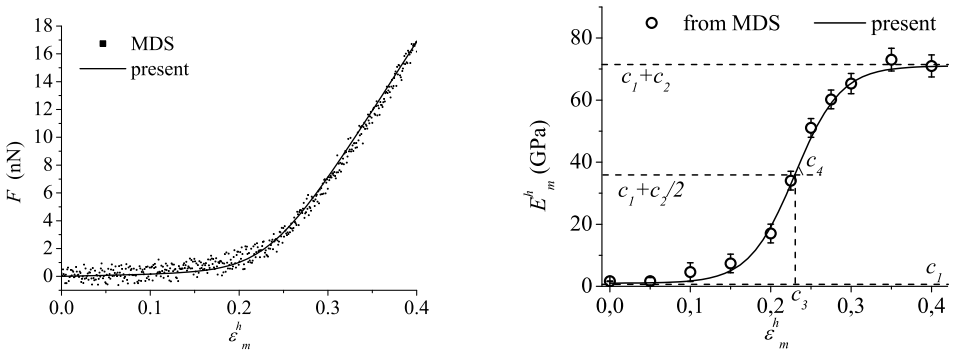

(a) (b)

Figure 2: Collagen $F-\varepsilon_m^h$ (a) and $E_m^h-\varepsilon_m^h$ (b) relationships obtained by MDS (Gautieri, Buehler, and Redaelli, 2009) and present model. Parameters: $\ell_c = 8.4$ nm, $\hat{E}_o = 1$ GPa, $\hat{E} = 70$ GPa, $k = 35$, $\varepsilon_o^h = 0.23$. MDS estimate of E_m^h has been obtained as the mean-values-based slope of F-ε_m^h. The asymptotic value at $\varepsilon_m^h \to -\infty$ is $c_1 = \hat{E}_o r_\ell$, the asymptotic value at $\varepsilon_m^h \to \infty$ is $c_1 + c_2$ where $c_2 = \hat{E} r_\ell$, the value at $\varepsilon_m^h = c_3 = \varepsilon_o^h / r_\ell$ is $c_1 + c_2/2$, and, finally, the slope of the curve at $\varepsilon_m^h = c_3$ is $c_4 = k c_2 r_\ell / 4$.

dressed. The transition mechanism from entropic to energetic regimes is highlighted in Fig. 3b where the tangent modulus is plotted versus the molecular extension. It is remarked that transition description is not governed by any phenomenological parameter and it straightly results from the solution of the equilibrium problem in Eq. 31. Therefore, transition evolution derives from the competition of the two stiffness E_m^s and E_m^h: when $E_m^s << E_m^h$ molecular mechanics is related only with entropic mechanism ($E_m \approx E_m^s$), when $E_m^s >> E_m^h$ only with energetic one ($E_m \approx E_m^h$), when $E_m^s \approx E_m^h$ with both mechanisms.

Soundness and effectiveness of the proposed approach for describing entropic-energetic transition are shown in Fig. 4a, where the computed strain rates $\dot{\varepsilon}_m^s$ and $\dot{\varepsilon}_m^h$ (normalized with respect to $\dot{\varepsilon}_m$) are plotted versus the molecular length ℓ_m. The figure refers to the case of a collagen molecule with $\ell_c = 301.7$ nm, for which MDS results by Buehler and Wong (2007) predicted that the entropic regime dominates for $\ell_m < 280$ and the energetic one for $\ell_m > 317$ nm. The computed strain rates are fully in agreement with this evidence ($\dot{\varepsilon}_m^h \to 0$ for $\ell_m < 280$ nm and $\dot{\varepsilon}_m^h \to 1$ for $\ell_m > 317$ nm). Thereby, since E_m^s has a pole at $\varepsilon_m^s = 1/r_\ell - 1$, equilibrium and compatibility conditions ensure that, when the nominal strain increases, ε_m^s increases and tends towards $1/r_\ell - 1$ but never reaches it ($\dot{\varepsilon}_m^s \to 0$ for $\ell_m > 317$ nm).

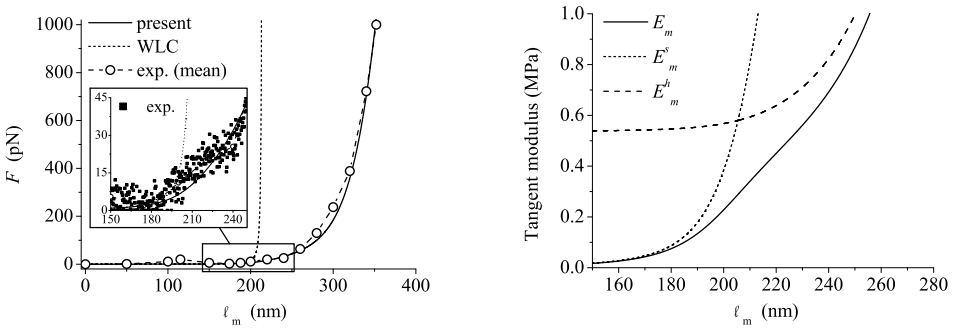

(a) (b)

Figure 3: (a) Collagen F-ℓ_m curves obtained by experimental tests (Bozec and Horton, 2005), classical WLC and present model. (b) Molecular (E_m), entropic (E_m^s), and energetic (E_m^h) tangent moduli vs. ℓ_m for collagen molecule. Parameters: $\ell_p = 14.5$ nm, $\ell_c = 215$ nm, $\hat{E}_o = 0.1$ GPa, $\hat{E} = 10$ GPa, $k = 10$, $\varepsilon_o^h = 0.65$, $\ell_{m,o} = 1$ nm.

Moreover, in Fig. 4b and as a further validation, the F-ℓ_m curve obtained in this latter case is successfully compared with the experimental data by Sun, Luo, Fertala, and An (2002) (available only for low molecular forces), as well as with the numerical results by Buehler and Wong (2007).

It is worth pointing out that a sensitivity study in the elastic regime has not been herein carried out. This is because the parameters for the entropic behavior are directly taken from the literature and WLC sensitivity has been widely investigated (Marko and Siggia, 1995; Holzapfel, and Ogden, 2010). On the other hand, model sensitivity in the energetic range can be retained as a trivial topic: the exponential function describing E_m^h is simple and characterized by physically-based governing parameters with a clear and straight effect on E_m^h (see Fig. 2b). Accordingly, only within the transition region between entropic and energetic elasticity, a sensitivity study may provide some non-trivial indications. Nevertheless, since nowadays experimental or computational MDS-based data on this issue are missing, such an analysis is left for future studies.

4.2 Molecular elasto-damage response

4.2.1 Force-induced damage

The elasto-damage response of over-stretched collagen molecules is also addressed by means of the predictive theory in Eq. 21, Eq. 22 and Eq. 23. In order to show

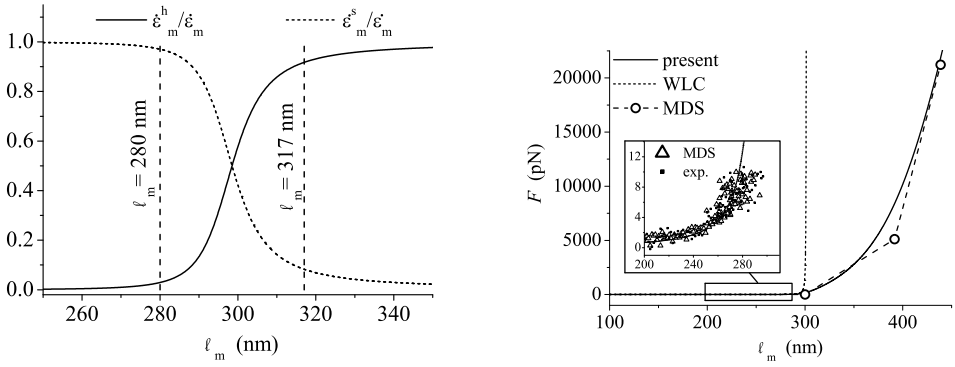

(a) (b)

Figure 4: (a) Strain rates associated with entropic ($\dot{\varepsilon}^s_m$) and energetic ($\dot{\varepsilon}^h_m$) mechanisms (normalized with respect to $\dot{\varepsilon}_m$) computed by the present approach. (b) Collagen F-ℓ_m curves obtained by experimental tests (Sun, Luo, Fertala, and An, 2002), MDS (Buehler and Wong, 2007), classical WLC, and present model. Parameters: $\ell_p = 16$ nm, $\ell_c = 301.7$ nm, $\hat{E}_o = 5$ GPa, $\hat{E} = 100$ GPa, $k = 10$, $\varepsilon^h_o = 0.35$, $\ell_{m,o} = 1$ nm.

model sensitivity, different damage rules (DR 1 and DR 2) and different values of damage-related parameters (c_m, v_o, and w_m) are considered. In this application no external damage sources are addressed ($a_m = 0$). Obtained results are compared with the ones from MDS by Buehler (2006) on small straight tropocollagen segments ($\ell_c = 8.4$ nm) where the tensile force is applied either to the three polypeptides (case 1) or to a single polypeptide strand (case 2). In order to reproduce the MDS assumptions, only energetic elasticity (the one related with damage) is addressed, and thereby $\ell_{m,o} \to \ell_c$. It is worth pointing out that the way the load is transferred to the molecule (through either three or one polypeptides) affects also the parameters governing the purely elasto-energetic response.

As it is clearly shown in Fig. 5, the model qualitatively and quantitatively agrees well with atomistic MDS computations. The physical meaning of damage-related parameters is clearly highlighted: w_m is directly proportional with the molecular ultimate strength, c_m and initial damage rate vary inversely, and v_o limits damage rate in DR 2. Moreover, the comparison between the results of present model and MDS suggests DR 2 to be more suitable than DR 1 for describing collagen damage behavior.

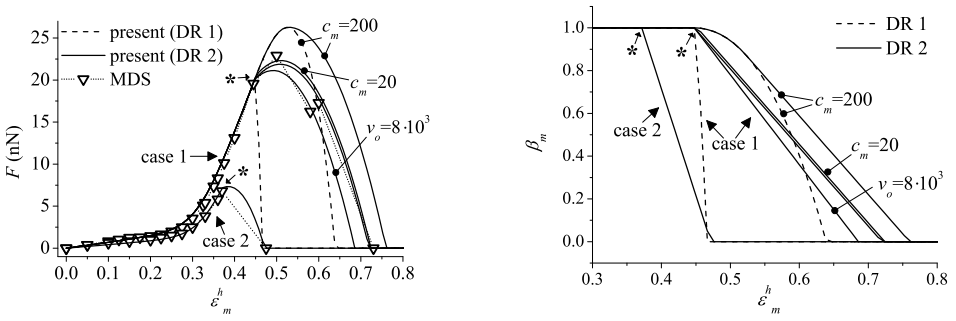

(a) (b)

Figure 5: Elasto-damage response of tropocollagen segments ($\ell_{m,o} \to \ell_c = 8.4$ nm) under traction loads applied either to the three polypeptides (case 1) or to a single polypeptide strand (case 2). Tensile force F (a) and damage parameter β_m (b) vs. ε^h_m obtained by present model for DR 1 (with different values of c_m [kPa · s]) and DR 2 (with different values of c_m [kPa · s] and v_o [s^{-1}]). The case 2 has been analyzed only by DR 2. In (a), MDS results by Buehler (2006) are also reported. Parameters case 1 (unless specified): $\hat{E}_o = 5$ GPa, $\hat{E} = 90$ GPa, $k = 32$, $\varepsilon^h_o = 0.31$, $w_m = 1.5$ GPa, $c_m = 1$ kPa · s, $v_o = 7 \cdot 10^3$ s^{-1}. Parameters case 2: $\hat{E}_o = 3$ GPa, $\hat{E} = 7.3$ GPa, $k = 35$, $\varepsilon^h_o = 0.31$, $w_m = 0.4$ GPa, $c_m = 1$ kPa · s, $v_o = 20 \cdot 10^3$ s^{-1}. Symbol * denotes damage onset.

4.2.2 Influence of non-mechanical damage sources

In order to assess the effects of non-mechanical damage sources and considering the following positive-valued constants $\dot{\ell}^o_m, a^o_m, t_i, t_o \in \mathbb{R}^+$, the following three case studies are considered

1. constant deformation rate and constant non-mechanical source of damage:

$$\dot{\ell}_m = \dot{\ell}^o_m, \quad a_m = -a_{m,o}; \tag{32}$$

2. constant deformation rate and impulsive (Gaussian shaped) non-mechanical source of damage:

$$\dot{\ell}_m = \dot{\ell}^o_m, \quad a_m = -a_{m,o} e^{-(t-t_i)^2/\mu^2}, \tag{33}$$

where t_i is the time interval between the beginning of the mechanical test and the time at which the maximum value of a_m is attained;

3. constant non-mechanical source of damage prior to a tensile test with constant deformation rate:

$$\dot{\ell}_m = \begin{cases} 0 & \text{for } t \le t_o \\ \dot{\ell}_m^o & \text{for } t > t_o \end{cases}, \quad a_m = \begin{cases} -a_{m,o} & \text{for } t \le t_o \\ 0 & \text{for } t > t_o \end{cases}, \tag{34}$$

where t_o is the time duration of the non-mechanical source of damage, as well as the time at which the mechanical test begins.

The physical interpretation of the three cases herein addressed is to mimic three realistic scenarios occurring in biological tissues: the tissue experiences a constant biochemical/electrical stimulus (non-mechanical damage source) during its mechanical functioning (case 1); the biochemical/electrical damage stimulus is high but short in time (for instance as in an instantaneous release of toxic molecules rapidly metabolized by cells, case 2); a biochemical/electrical stimulus occurs during tissue rest and, then, the tissue is stretched (case 3).

Referring to the DR 2 case ($\dot{\beta}_m$ is lower-bounded by $-v_o$), Fig. 6 shows the evolution of ε_m^h and a_m in the three case studies. Moreover, Fig. 7a highlights the comparison for the $F - \varepsilon_m^h$ relationships with the reference condition $a_m = 0$.

A complex coupling between non-mechanical and mechanical-related damage sources arises. Addressing cases 1 and 2, the $F - \varepsilon_m^h$ curve shows an initial slope coincident with the purely mechanical case. In case 1, when the mechanical energetic strain energy Ψ_m^h reaches the reduced threshold value $w_m - |a_m|$, damage occurs inducing the reduction of the molecular apparent elastic modulus. The damage onset strain varies inversely with the value of $a_{m,o}$. As regards case 2, damage increases during the non-mechanical source impulse but, when $a_m \to 0$, damage evolution stops (see Fig. 7b) until Ψ_m^h is equal to the threshold w_m. In fact, since Ψ_m^h is a single-valued function of ε_m^h, the strain level corresponding to the mechano-regulated damage onset coincides with the reference case. The decrease in the molecular apparent elastic modulus (i.e., the damage increase) is directly proportional with both the impulse height and the time exposition to the damage source, the first effect being mitigated by the fact that the damage rate is bounded by v_o, and the second is related only with the time interval in which $\Psi_m^h - a_m - w_m > 0$. Addressing case 3, the apparent initial modulus is lower than the reference case since the molecule is initially damaged. The amount of damage in the undeformed state ($\varepsilon_m = 0$) directly depends on the time exposition to the non-mechanical source and highly affects the mechanical response. The mechanism governing the mechano-regulated damage is similar to the case 2.

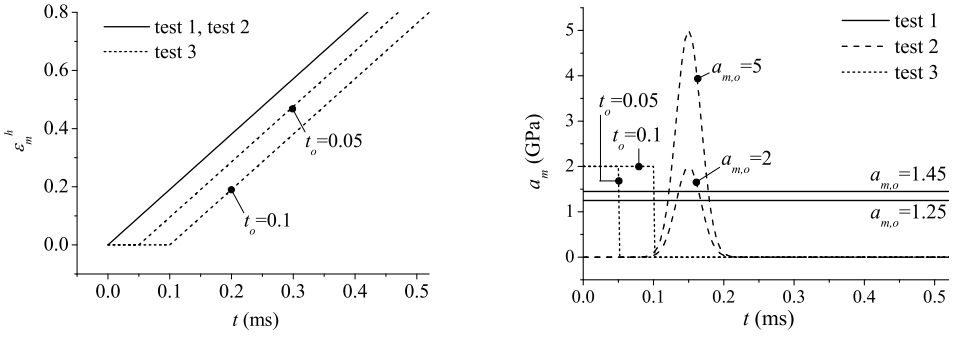

(a) (b)

Figure 6: Time evolution of ε_m^h and a_m [Nm] for test 1, 2 and 3. Parameters: $\dot{\ell}_m^o = 1$ mm/min, $t_i = 0.15$ ms, $\mu = 0.025$ ms.

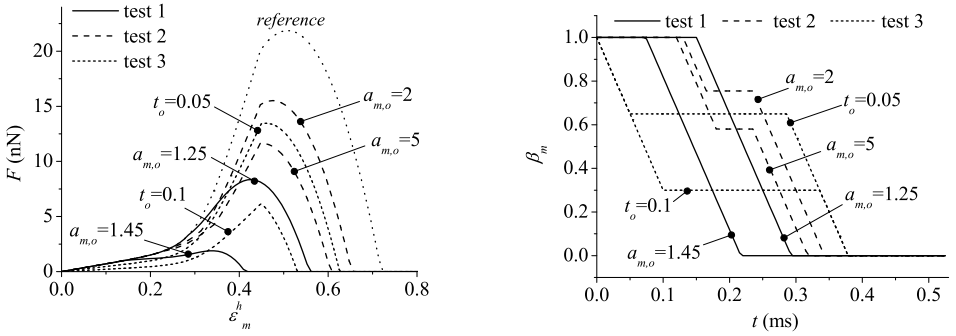

(a) (b)

Figure 7: Elasto-damage response of tropocollagen segments ($\ell_{m,o} \to \ell_c = 8.4$ nm) under traction loads and non-mechanical damage sources. Tensile force F vs. ε_m^h (a) and damage parameter β_m vs. t (b) obtained by present model with DR 2 for three case studies ($\dot{\ell}_m^o = 1$ mm/min, $t_i = 0.15$ ms, $\mu = 0.025$ ms). Parametric analyses varying $a_{m,o}$ [Nm] (for cases 1 and 2) and t_o [ms] (for case 3). In (a), the reference result without non-mechanical damage sources is also reported. Constant parameters: $\hat{E}_o = 5$ GPa, $\hat{E} = 90$ GPa, $k = 32$, $\varepsilon_o^h = 0.31$, $w_m = 1.5$ GPa, $c_m = 1$ kPa $\cdot$ s, $v_o = 7 \cdot 10^3$ s^{-1}.

5 Conclusions

In this paper an internal constrained approach based on convex analysis has been employed for developing an elasto-damage model able to describe the mechani-

cal behaviour of biopolymer molecules. The analytical formulation is derived by combining equilibrium and constitutive laws at the nanoscale, the first being obtained by applying the Principle of Virtual Powers, and the second defined by suitable expressions for free-energy and pseudo-potential of dissipation. The model is formulated in agreement with well-established both experimental and numerical atomistic evidences, resulting dependent on few parameters with a clear physical meaning. Moreover, as confirmed by the numerical applications herein discussed in the case of collagen, proposed approach is able to describe many complex mechanisms highly affecting fundamental processes in molecular biology and biomechanics: nonlinearly elastic behavior due to entropic and energetic mechanisms; transition between these two mechanisms and their mutual interaction; damage evolution induced by molecular overstretching or non-mechanical damage source. Such a predictive theory is based on a non classical but simple analytical formulation, allowing to develop continuum-based models of biological structures. In the case of soft collagenous tissues, present formulation might be straightforwardly integrated in the structural multiscale approach recently proposed (Maceri, Marino, and Vairo, 2010a) and applied (Maceri, Marino, and Vairo, 2010b, 2012; Marino and Vairo, 2012) by the authors. Moreover, the alteration of model parameters' value related to unconventional nanoscale causes (e.g., related to genetic defects, mechano-biological stimuli, biochemical agents, electromagnetical actions) might be investigated by means of computational atomistic techniques and, hopefully, by nanoscale experimental results. This opens to possible groundbreaking applications where such nanoscale mechanisms might be upscaled for investigating their effects at the macroscale.

Acknowledgement: This work was developed within the framework of the Lagrange Laboratory, a European research group comprising CNRS, CNR, the Universities of Rome "Tor Vergata", Calabria, Cassino, Pavia and Salerno, Ecole Polytechnique, University of Montpellier II, ENPC, LCPC and ENTPE.

References

Ayton, G.S.; Voth, G.A. (2010): Multiscale simulation of protein mediated membrane remodeling. *Seminars in Cell & Developmental Biology*, vol. 21, pp. 357-362.

Bozec, L.; Horton, M. (2005): Topography and mechanical properties of single molecules of type I collagen using atomic force microscopy. *Biophysical Journal*, vol. 88, pp. 4223-4231.

Buehler, M.J. (2006): Atomistic and continuum modeling of mechanical properties of collagen: Elasticity, fracture, and self-assembly. *Journal of Material Research*, vol. 21, pp. 1947-1961.

Buehler, M.J.; Wong, S.Y. (2007): Entropic Elasticity Controls Nanomechanics of Single Tropocollagen Molecules. *Biophysical Journal*, vol. 93, pp. 37-43.

Buehler, M. J.; (2008). Nanomechanics of collagen fibrils under varying cross-link densities: atomistic and continuum studies. *Progress in Materials Science*, vol. 53, pp. 1101-1241.

Comninou, M.; Yannas, I.V. (1976): Dependance of Stress-Strain Nonlinearity of Connective Tissues on the Geometry of Collagen Fibers. *Journal of Biomechanics*, vol. 9, pp. 427-433.

de Leeuw, N.H. (2004): Resisting the Onset of Hydroxyapatite Dissolution through the Incorporation of Fluoride. *Journal of Physical Chemistry B*, vol. 108, pp. 1809-1811.

Fratzl, P. (2008): *Collagen: structure and mechanics*. Springer, Berlin.

Freed, A.D.; Doehring, T.C. (2005): Elastic model for crimped collagen fibrils. *Journal of Biomechanical Engineering*, vol. 127, pp. 587-593.

Frémond, M. (2002): *Non-smooth thermomechanics*. Springer-Verlag, Berlin.

Fung, Y.C. (1981): *Biomechanics – Mechanical properties of living tissues*. Springer, New-York.

Gautieri, A.; Buehler, M.J.; Redaelli, A. (2009): Deformation rate controls elasticity and unfolding pathway of single tropocollagen molecules. *Journal of the Mechanical Behavior of Biomedical Materials*, vol. 2, pp. 130-137.

Hansen, K.A.; Weiss, J.A.; Barton, J.K. (2002): Recruitment of Tendon Crimp With Applied Tensile Strain. *Journal of Biomechanical Engineering*, vol. 124, pp. 72-77.

Holzapfel, G.A.; Gasser, T.C.; Stadler, M. (2002): A structural model for the viscoelastic behavior of arterial walls: Continuum formulation and finite element analysis. *European Journal of Mechanics - A/Solids*, vol. 21, pp. 441-63.

Holzapfel, G.A.; Gasser, T.C.; (2007): Computational stress-deformation analysis of arterial walls including high-pressure response. *International Journal of Cardiology*, vol. 116, pp. 78-85.

Holzapfel, G.A.; Ogden, R.W. (2010): On the Bending and Stretching Elasticity of Biopolymer Filaments. *Journal of Elasticity*, vol. 104, pp. 319-342.

Humphrey, J.D. (2002): *Cardiovascular Solid Mechanics. Cells, Tissues, and Organs*. Springer-Verlag, New York.

Jackson, S.P.; Bartek, J. (2009): The DNA-damage response in human biology and disease. *Nature*, vol. 461, pp. 1071-1078.

Linke, W.A.; Ivemeyer, M.; Mundel, P.; Stockmeier, M.R.; Kolmerer, B. (1998) Nature of PEVK-titin elasticity in skeletal muscle. *Proceedings of the National Academy of Sciences of the USA*, vol. 95, pp. 8052-8057.

Maceri, F.; Marino, M.; Vairo, G. (2010a): A unified multiscale mechanical model for soft collagenous tissues with regular fiber arrangement. *Journal of Biomechanics*, vol. 43, pp. 355-363.

Maceri, F.; Marino, M.; Vairo, G. (2010b): From cross-linked collagen molecules to arterial tissue: a nano-micro-macroscale elastic model. *Acta Mechanica Solida Sinica*, vol. 23(S1), pp. 98-108.

Maceri, F.; Marino, M.; Vairo, G. (2012):An insight on multiscale tendon modeling in muscle- tendon integrated behavior. *Biomechanics and Modeling in Mechanobiology*, vol. 11, pp. 505-517.

Marino, M.; Vairo, G. (2012): Stress and strain localization in stretched collagenous tissues via a multiscale modeling approach. *Computer Methods in Biomechanics and Biomedical Engineering*, doi: 10.1080/10255842.2012.658043.

MacKintosh, F.C.; Käs, J.; Janmey, P.A. (1995): Elasticity of Semiflexible Biopolymer Networks. *Physical Review Letters*, vol. 75, pp. 4425-4428.

Marko, J.F.; Siggia, E.D. (1995): Stretching DNA. *Macromolecules*, vol. 28, pp. 8759-8770.

Moreau, J.J. (2003): *Fonctionnelles convexes*. Editions of Department of Civil Engineering, University of Rome Tor Vergata, ISBN 9788862960014, Roma.

Pagán, R.; Mackey, B. (2000): Relationship between Membrane Damage and Cell Death in Pressure-Treated Escherichia coli Cells: Differences between Exponential- and Stationary-Phase Cells and Variation among Strains. *Applied and Environmental Microbiology*, vol. 66, pp. 2829-2834.

Pichler, B.; Hellmich, C. (2011) Upscaling quasi-brittle strength of cement paste and mortar: A multi-scale engineering mechanics model. *Cement and Concrete Research*, vol. 41, pp. 467-476.

Pradhan, S.M.; Katti, D.R.; Katti, K.S. (2011): Steered Molecular Dynamics Study of Mechanical Response of Full Length and Short Collagen Molecules, *Journal of Nanomechanics and Micromechanics*, vol. 1, pp. 104-110.

Rawicz, W.; Olbrich, K.C.; McIntosh, T.; Needham, D.; Evans, E. (2000) Effect of Chain Length and Unsaturation on Elasticity of Lipid Bilayers. *Biophysical Journal*, vol. 79, pp. 328-339.

Sasaki, N.; Odajima, S. (1996): Elongation mechanism of collagen fibrils and force-strain relations of tendon at each level of structural hierarchy. *Journal of Biomechanics*, vol. 29, pp. 1131-1136.

Screen, H.R.C.; Lee, D.A.; Bader, D.L.; Shelton, J.C. (2004): An investigation into the effects of the hierarchical structure of tendon fascicles on micromechanical properties. *Proceedings of the Institution of Mechanical Engineers - Part H: Journal of Engineering in Medicine*, vol. 218, pp. 109-119.

Sun, Y.L.; Luo, Z.P.; Fertala, A.; An, K.N. (2002): Direct quantification of the flexibility of type I collagen monomer. *Biochemical and Biophysical Research Communications*, vol. 295, pp. 382-386.

Unnikrishnan, G.U.; Unnikrishnan, V.U.; Reddy, J.N. (2007): Constitutive material modeling of cell: a micromechanics approach. *Journal of Biomechanical Engineering*, vol. 129, pp. 315-323.

Wang, M.D.; Yin, H.; Landick, R.; Gelles, J.; Block, S.M. (1997): Stretching DNA with Optical Tweezers. *Biophysical Journal*, vol. 72, pp. 1335-1346.